Journal of Medical and Biological Engineering
https://doi.org/10.1007/s40846-026-01016-y

ORIGINAL ARTICLE

Green Synthesis of Gold Nanoparticles Using *Aronia Melanocarpa* and their Interaction with Melanin

Güleycan Dedecengiz Varol[1,2] · **Sakip Önder**[1] · **Görke Gürel Peközer**[1]

Received: 23 September 2025 / Accepted: 1 February 2026
© Taiwanese Society of Biomedical Engineering 2026

Abstract

Purpose Gold nanoparticles (AuNPs) have attracted significant attention in biomedical research due to their unique optical and electronic properties, making them suitable for biosensing, drug delivery, and imaging applications. This study explores the green synthesis of AuNPs using *Aronia melanocarpa*, a fruit rich in polyphenols and anthocyanins, which has not been previously reported in the literature for gold nanoparticle synthesis. Given that melanin is a critical biomarker for melanoma progression, we investigated the interaction between melanin and AuNPs synthesized with green chemistry methods.

Methods AuNPs were synthesized using aronia extract as reducing/stabilizing agent. The interaction between AuNPs and melanin was investigated using UV-Visible (UV-VIS) spectrophotometry and fourier transform infrared spectroscopy (FTIR) to assess their potential applications in bioanalysis.

Results The study confirms the interaction of AuNPs with melanin which is a pigment with a high potential to be used in biomedical applications including melanoma detection and biosensors. Changes in absorbance and spectral shifts suggest a strong interaction between melanin and AuNPs, particularly in acidic environments, indicating potential for use in diagnostic or sensing applications.

Conclusion This research demonstrates a cost-effective and eco-friendly method for AuNP synthesis and highlights its potential in melanin-related studies and broader biomedical applications.

Keywords Gold nanoparticles · Melanin · Green chemistry · Aronia melanocarpa

1 Introduction

Gold nanoparticles (AuNPs) are nanomaterials with versatile applications in biology. Thanks to their high surface area and easily processable surface properties, they are used for targeted drug delivery and genetic material delivery [1, 2]. They also play a role in medical diagnostics and therapeutic applications, such as destroying cancer cells with photothermal therapy and as imaging biomolecules. While improving diagnostic and therapeutic processes in biosensors and immunological applications, the unique optical and electronic properties of gold nanoparticles provide significant advantages in biomedical research.

AuNP synthesis methods involve (1) the reduction of gold ions (Au^{3+}) into AuNPs (Au^{0}) and (2) the stabilization of the particles [3]. AuNPs can be synthesized using physical, chemical, and biological methods. The synthesis methods usually employ three components: a metal precursor, reducing agent, and stabilizing/capping agents. The first and most widely preferred chemical method for the synthesis is Turkevich method which uses citrate as both reducing and stabilizing agent. Physical methods involve the use of ultrasound, microwave, laser ablation, electrochemical and photochemical reduction methods [4].

The biological synthesis also called green synthesis use plant extracts, fungi or microorganisms as reducing agents and stabilizers for the preparation of gold nanoparticles. This approach is an eco-friendly and non-toxic method. Plants are one of the most widely used natural materials for the biosynthesis of gold nanoparticles. Plant extracts contain natural compounds such as polyphenols, flavonoids,

✉ Görke Gürel Peközer
gpekozer@yildiz.edu.tr

[1] Department of Biomedical Engineering, Yildiz Technical University, Istanbul, Türkiye

[2] Department of Bioengineering, Yildiz Technical University, Istanbul, Türkiye

Published online: 16 February 2026

terpenoids, alkaloids and other biomolecules that are essential for reducing gold ions [5–8]. For instance, there are studies in the literature using plants such as green tea, eucalyptus, ginger, aloe vera and turmeric for gold nanoparticle synthesis [9–13].

Aronia melanocarpa, a fruit with high antioxidant capacity and abundant in polyphenols and anthocyanins, has notable health benefits, including immune support, cardiovascular protection, and anti-inflammatory effects [14, 15]. However, its potential for green synthesis of AuNPs remains unexplored.

The melanin pigment is produced by melanocytes scattered in the basal layer of the skin's epithelial covering known as the epidermis. In addition to giving color to the skin, hair and eyes, melanin plays a role in preventing skin cancer by protecting against the harmful rays of the sun [16, 17]. It provides pigmentation to cells, absorbs UV rays and can prevent cellular damage that can be caused by UV light exposure [18]. Melanin, which is found in nature in marine organisms such as cuttlefish (sepia officinalis), octopus, squid and also in bacteria, can also be obtained biosynthetically [19–22]. Melanin was incorporated into multimodal imaging nanoplatforms by binding with Cu^{2+} and Fe^{3+} for use in positron emission tomography (PET) and magnetic resonance imaging (MRI) [23, 24].

As with the Cu^{2+} and Fe^{3+} ions, melanin's metal chelating ability is well known [25, 26]. Abnormal production of melanin is linked with several conditions such as Parkinson's disease, albinism, melasma, melanoma, vitiligo and aging thus, can act as a potential biomarker for diagnostics [27–32]. Therefore, the sensitive, selective, and straight forward detection method for melanin is critical for in-depth understanding, diagnosis, and proper management of hypo and hyperpigmented disorders [33].

The unique properties of AuNPs suggest that they could interact with melanin in ways that enhance the diagnosis and treatment of diseases. In this study, it is aimed to sensitively detect the amount of melanin using gold nanoparticles that can be easily and cheaply synthesized from aronia fruit by green synthesis method. TEM analysis was performed to obtain shape and size information of the synthesized AuNPs. The optical properties of AuNP and also the effect of melanin concentration and pH on these nanoparticles was investigated in UV-visible (UV-VIS) spectrophotometer. Aronia extract, melanin, synthesized AuNPs and their interaction with melanin were analyzed by fourier transform infrared spectroscopy (FTIR) to determine the chemical bonds and functional groups that are involved in the interaction. This study is a preliminary report that shows *Aronia melanocarpa*, with its known high polyphenol and anthocyanin content, is a good reducing/stabilizing agent for AuNPs synthesis. The study also shows AuNPs synthesized with this method can interact with melanin. The interaction of AuNPs with melanin can have broad applications in diagnosis of melanoma, development of biosensors, pharmaceutical testing and advanced therapeutics.

2 Experimental

2.1 Materials

Aronia Melonacarpa was bought from the greengrocer. Gold (III) Chloride Trihydrate ($HAuCl_3.3H_2O$) was obtained from SIGMA-ALDRICH (16961-25-4). Melanin was extracted and purified from the Cuttlefish ink sold by the Nortindal brand. HCI and NaOH were purchased from ISOLAB.

2.2 Methods

2.2.1 Synthesis of AuNPs from Aronia Extract

Aronia fruits were thoroughly washed and cleaned of dust and impurities by first tap water and then distilled water and left to dry at room temperature. The fruits were blended into small pieces using a kitchen type blender without adding water. 1 g of the frozen aronia puree was taken and mixed with 20 ml of water. The mixture was filtered using a Grade 1 Whatman paper filter. This filtered aronia extract was mixed with 60 µL of 0.03 wt% gold (III) chloride trihydrate solution (in distilled water) and stirred on a magnetic stirrer for 1 h at RT. The mixed solution was then filtered through 0.02 µm syringe filter and the filtrate was sonicated with a probe sonicator for 2 min with 30% efficiency.

2.2.2 Spectrophotometric Characterization of AuNPs

Absorbance of AuNPs was analyzed by spectrophotmetrical methods. Spectrophotometric behaviour of AuNPs at different pH values was also investigated. pH of gold nanoparticle solutions were adjusted using 0.1 M HCl and NaOH solutions. Absorbance scan between 350 and 800 nm were performed in UV-VIS spectrophotometer using quartz cuvettes and appropriate blank solutions.

2.2.3 Transmission Electron Microscopy (TEM) Analysis of AuNPs

AuNP solutions were spotted onto TEM grids, dried prior to imaging and the images were acquired at varying magnifications by using TEM (JEM2100 PLUS, Jeol).

2.2.4 Melanin Isolation

For the extraction of melanin from cuttlefish ink, the method in a previous study was applied [34]. 750 µL of distilled water was added to 500 µL of the ink and taken into centrifuge tubes. These solutions were mixed by vortexing and centrifuged at 15,000 rpm for 5 min. The supernatant formed after centrifugation was removed from the tube. This step was repeated twice by adding 1 ml of distilled water to the pellet and centrifuging again at the same speed and time. After the third centrifugation step, the remaining pellet was transferred to petri dishes. The melanin in the petri dishes was kept in the oven at 50 °C for 2 days to get dry form. Dried melanin powder was weighed and melanin solutions with concentrations of 1%, 0.75%, 0.25% and 0.05% were prepared in distilled water.

2.2.5 Investigation of Interaction between AuNPs and Melanin

250 µL of distilled water was added to 250 µL of AUNP solution. To investigate how the interaction is affected at different pH values, 5 µL of melanin solution at various concentrations was mixed with different volumes (20, 50, 100 µL) of HCl and NaOH to adjust the medium pH. The interaction was studied by spectrophotometry and FTIR analyzes.

2.2.5.1 Spectrophotometric Analysis Spectrophotometric analyzes were performed to observe a shift or change in the absorbance spectra of AuNPs upon melanin interaction. The analysis was performed using a UV-VIS spectrophotometer in the wavelength range of 350–800 nm for AuNPs at different pH values containing different concentrations of melanin. AuNP concentration was kept constant to ensure that the change in absorbance was solely a function of the melanin concentration.

2.2.5.2 FTIR Analysis FTIR analysis was also performed to examine the chemical bonds and functional groups involved in the interaction. Samples containing AuNP and melanin at different concentrations were dried in an oven at 37 °C to be used in FTIR analysis. The functional groups and possible interactions between AuNP and melanin were characterized using FTIR device and performed in the wavelength range of 4000–1000 cm^{-1}.

2.2.5.3 Statistical Analysis A linear regression analysis was conducted using the ordinary least squares (OLS) method to establish a calibration curve and define the quantitative relationship between melanin concentration and absorbance. The statistical parameters calculated included the coefficient of determination (R^2) to assess the goodness of fit and a one-sample t-test to determine the p-value for the statistical significance of the correlation slope. A p-value of less than 0.05 was utilized as the threshold for statistical significance to validate the sensitivity of the AuNP-based melanin detection.

3 Results and Discussion

3.1 Synthesis of AuNPs from Aronia Extract

When Au^{3+} was reduced to Au^0 in in aronia extract, color change of the solution was observed with the naked eye. The red-purple solution, which was lighter in color before mixing, became darker as AuNPs form (Fig. 1). Color change provides the first evidence that Au NPs were synthesized.

When examined at different pH values from acidic to basic, it was clearly seen that the color of these solutions

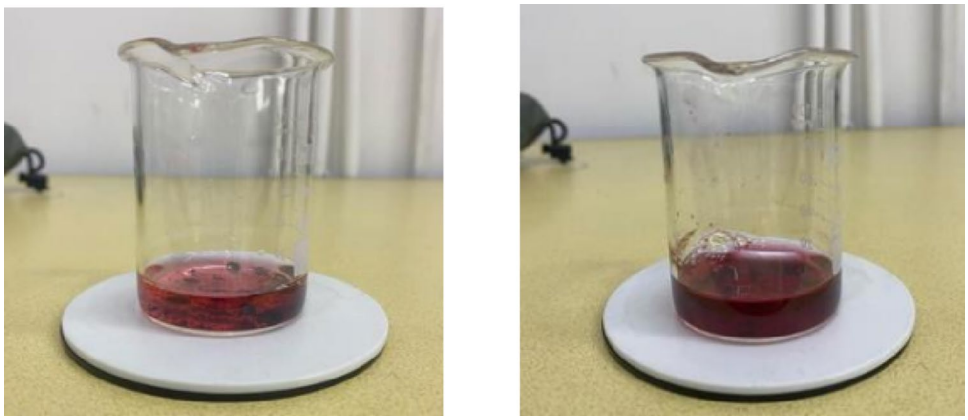


Fig. 1 Color of the solution pre-stirring (left) and post-stirring (right) during AuNP synthesis

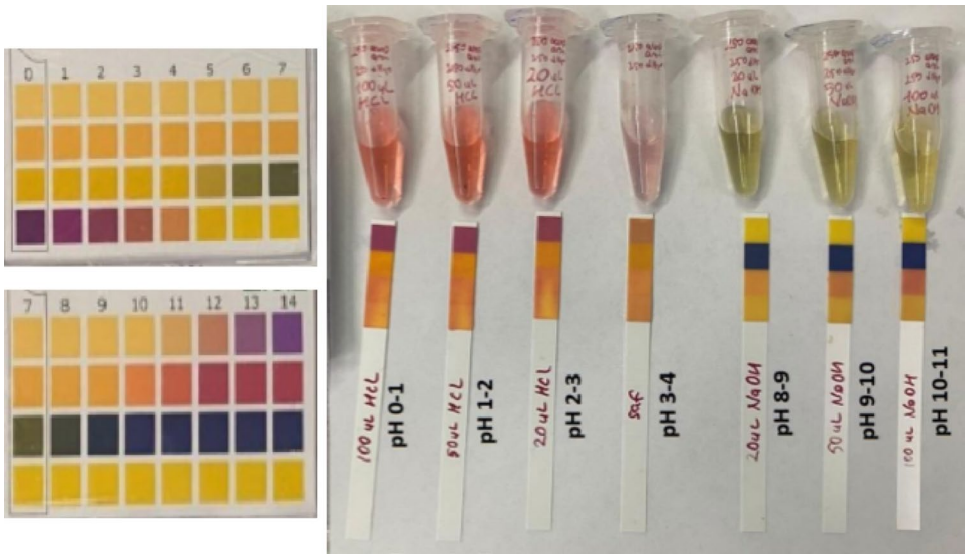


Fig. 2 Color change of AuNPs at different pH values

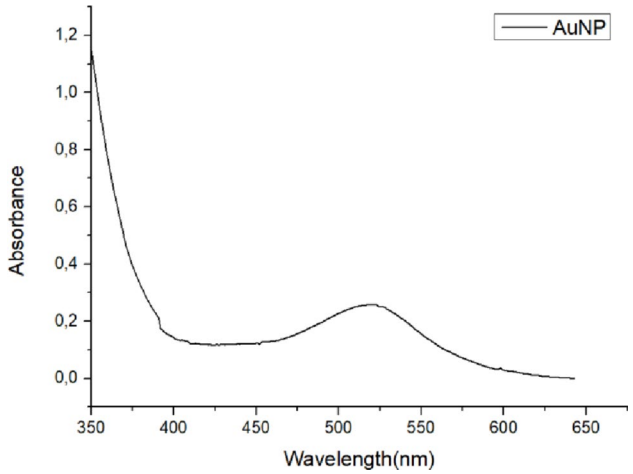


Fig. 3 Absorbance value of AuNP

was changed from red to green (Fig. 2). Gold nanoparticles generally remain stable in acidic media because the nanoparticles repel each other and are uniformly dispersed in solution [35]. In this case, the surface plasmon resonance (SPR) peak of gold nanoparticles is in the red region of the visible spectrum [36]. Therefore, the colour of the solution is observed as red. In basic media, nanoparticles may experience a change in their surface charge. Neutralization of charges can cause nanoparticles to aggregate. The aggregation of nanoparticles increases their size and leads to shifts in the surface plasmon resonance peak. As the nanoparticle size increases, the SPR peak shifts towards longer wavelengths and the solution becomes green or blue-green in colour [37].

3.2 Spectrophotometric Analysis of AuNPs

When the wavelength scan was performed for the synthesized AuNP, the maximum absorbance peak was observed at 522 nm (Fig. 3). The observed peak is consistent with established literature, which reports that AuNPs exhibit a characteristic surface plasmon resonance (SPR) band between 500 and 550 nm [38, 39].

Since the color of the gold nanoparticle solutions shifts in different pH conditions, the spectral behavior of the particles was also measured (Fig. 4). When the absorbance spectra of the synthesized AuNPs under alkaline conditions are analyzed, the absorption bands are observed to broaden, with the peaks exhibiting a red shift toward 600 nm at pH levels 8–9. As the pH increases further to the range of 9–11, the peak gradually diminishes and eventually disappears [40]. An additional peak towards 350–400 nm also appeared in increasing pH conditions.

In Fig. 4b, it is seen that the absorbance spectra shows a blue shift towards 500 nm for ph 1–3 interval and then comes back to 522 at pH 0–1 interval. Absorbance also increases and the peak gets sharper at pH 0–1 condition.

Changes in pH can affect the optical properties of gold nanoparticles by inducing aggregation, which in turn alters their surface plasmon resonance (SPR) characteristics. This resonance results from the interaction of free electrons of gold nanoparticles with light. Factors such as the size, shape, refractive index, chemical properties and pH of the surrounding medium affect the wavelength at which this resonance occurs [41, 42]. Ligands in the aronia extract that stabilize the gold nanoparticles can be protonated and deprotonated changing the charge distribution on the surface of the nanoparticles. Low pH values the repulsive forces between AuNPs can be stronger preventing the aggregation

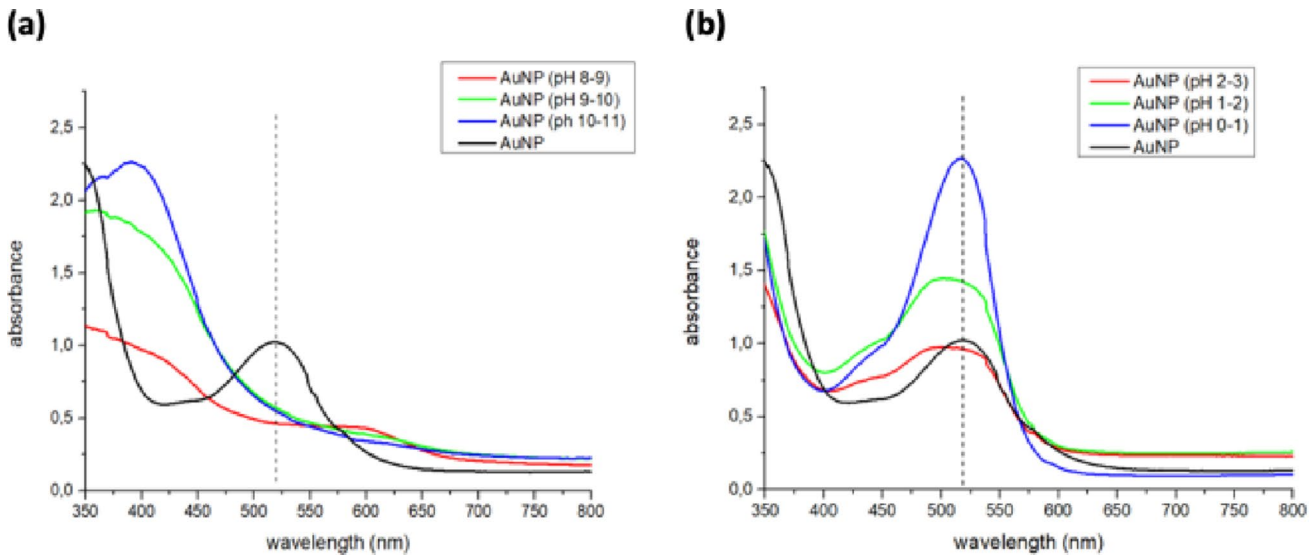


Fig. 4 Absorbance graph of AuNP under alkaline conditions (**a**), under acidic conditions (**b**)

of nanoparticles resulting in smaller size particles showing high absorbance and sharper peaks. The prominent shift towards longer wavelengths observed in Fig. 4a is likely attributable to the pH-induced aggregation of gold nanoparticles into larger clusters.

In the literature, there is a consensus on the effect of pH on the efficiency of AuNP formation and size of AuNPs formed. It is discussed that at acidic pH, the reducing agent is less reactive since protons stabilize it, lowering its electron-donating ability. Thus, reduction is slower. Low reduction rate decreases the number of nucleation events, leading to fewer nuclei. Because there are fewer nuclei, the available Au^0 atoms preferentially deposit on these limited seeds, allowing them to grow larger. Therefore, gold nanoparticles grow larger. In contrast, higher pH accelerates reduction, increases nucleation frequency, and promotes the formation of smaller nanoparticles. Besides at higher pH, capping/stabilizing agents are more ionized, providing better electrostatic stabilization against aggregation. This favors the preservation of small, discrete nanoparticles [43–47].

Once the particles are formed, the effect of pH on AuNP stability and hydrodynamic size depends on the capping agents that stabilize the particles and prevent them from aggregation. Although certain compounds such as fatty acids, carbohydrates, proteins and polyphenols are suggested to have capping and stabilizing activity in the green synthesis of nanoparticles, the specific phytochemicals responsible for these roles in our study remain unclear [48–50]. However, the results indicate that acidic pH may have favored stability through protonated functional groups on the capping agents and stabilizing agents present in the Aronia extract, while basic pH often promoted aggregation and larger assemblies.

3.3 TEM Analysis of AuNPs

TEM analysis revealed that Aronia extract induced synthesis formed roughly spherical AuNPs with diameters ranging from 10 to 20 nm (Fig. 5). These results are consistent with the results in the literature. In the study conducted by Verma et al., in which gold nanoparticles were obtained by the citrate reduction method, the colloidal gold particles were reported to have an average diameter of approximately 18 nm, with only a small number of particles deviating from this size. The TEM analysis further confirmed that the particles were monodispersed [35]. The particle size of AuNPs formed by the reduction of gold ion by the bacterial cell supernatant of *P. aeruginosa ATCC 90,271* was found to be 15 ± 5 by Husseiny et al. [51]. TEM image of gold nanoparticles synthesized by Ankamwar using leaf extract of Terminalia Catappa as reducing and stabilizing agent shows that the morphology of gold nanoparticles is mostly spherical, their size varies from 10 to 35 nm and the average size is about 21.9 nm [52].

3.4 Analysis of Interactions with AuNPs and Melanin

Interaction of gold nanoparticles with melanin was also studied by investigating the absorbance spectra of AuNPs after melanin addition to the solution (Fig. 6). A decrease in the absorbance of AuNPs is observed after its interaction with melanin (Fig. 6a). At basic pH values the behaviour of absorbance peaks of gold nanoparticles and melanin were very similar to the peaks of gold nanoparticles at basic pH (Fig. 4a) suggesting the absence of interaction between gold nanoparticles at basic pH values. In basic conditions,

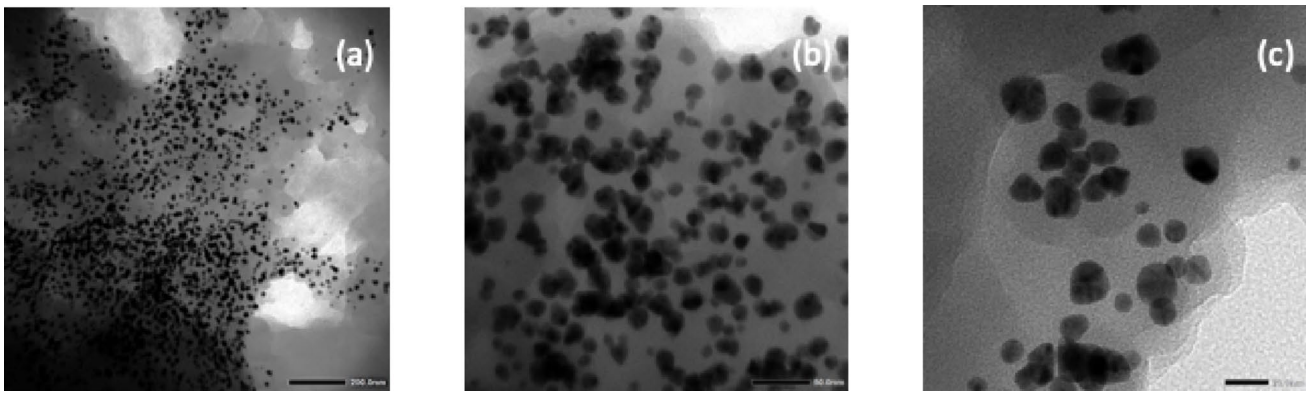


Fig. 5 TEM images of AuNPs (**a**) 20kX (**b**) 80kX (**c**) 150 kX. Scale bar shows 200 nm, 50 nm and 20 nm respectively

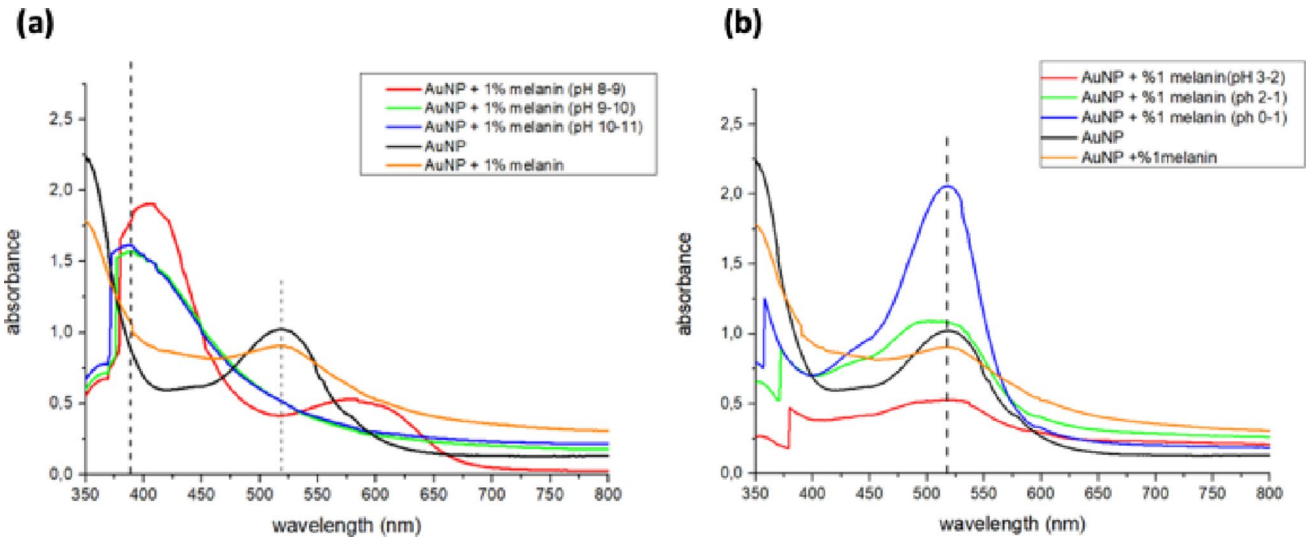


Fig. 6 Absorbance graph of AuNP and melanin interaction under different basic conditions (**a**), under different acidic conditions (**b**). pH of the AUNP group is between 3–4 as it can be seen in the Fig. 2

melanin tends to deprotonate which results in an increased negative charge on its surface due to deprotonation of functional groups like carboxyl (-COOH) and hydroxyl (-OH) groups [53, 54]. This negative charge could lead to electrostatic repulsion between melanin and the AuNPs preventing them from interacting.

However, we observed a decrease in absorbance without a shift in the peak in acidic environment. The binding of gold nanoparticles on melanin might have reduced the efficiency in light absorption by the nanoparticle surface, possibly resulting in less effective plasmonic excitation. In acidic environment, gold nanoparticles are more dispersed and nonaggregated. On the other hand, melanin becomes protonated which reduces its negative charge [54]. The decreased charge density on melanin might weaken the electrostatic repulsion between melanin and the nanoparticles enhancing their interactions.

At low pH, damping of gold nanoparticles' absorbance due to interactions with melanin is also concentration dependent. The absorbance decreased as the melanin concentration increased (Fig. 7). When gold nanoparticles adsorb onto melanin, they are likely removed from the free nanoparticle pool in solution decreasing the free AuNP concentration. As more nanoparticles adsorb to melanin, fewer nanoparticles remain dispersed in the solution, which could lead to a decrease in the overall number of free nanoparticles that are able to absorb light at 550 nm. This would result in a decrease in absorbance as melanin concentration increases.

To assess the linearity of the relationship between melanin concentration and absorbance, we plotted the melanin concentration vs. lambda max graph (Fig. 8). We observed a clear linear relation indicating that as more AuNPs adsorb onto the melanin surface, they are removed from the free nanoparticle pool, leading to a linear decrease in the measured light absorption at the SPR peak. The negative linear relationship between melanin concentration and the absorbance of AuNPs is statistically significant at a 95%

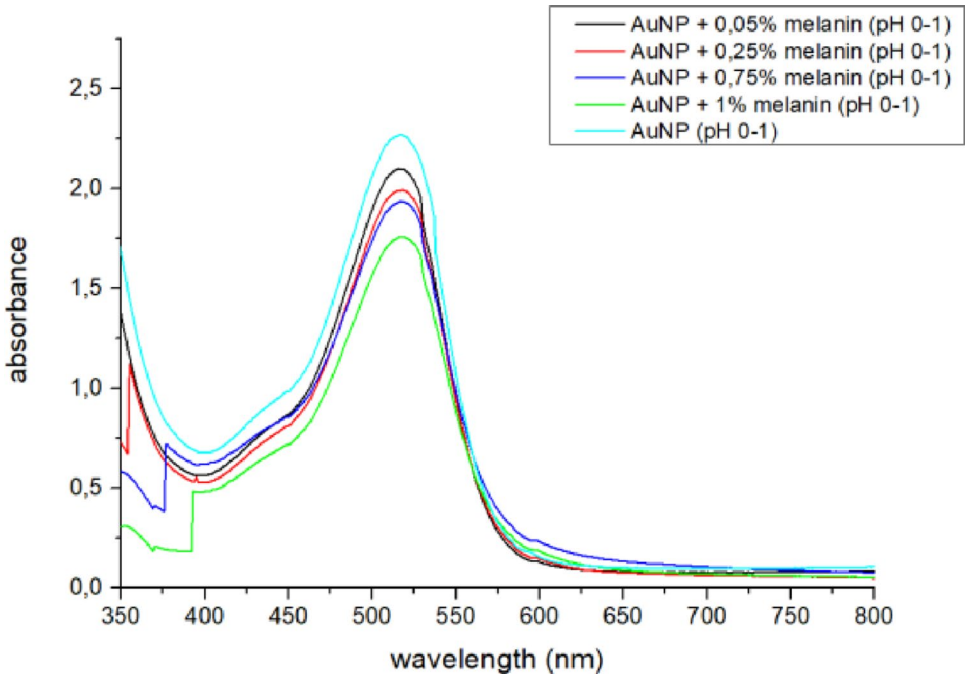


Fig. 7 Absorbance graph of AuNP with different melanin concentrations at pH 0–1 condition

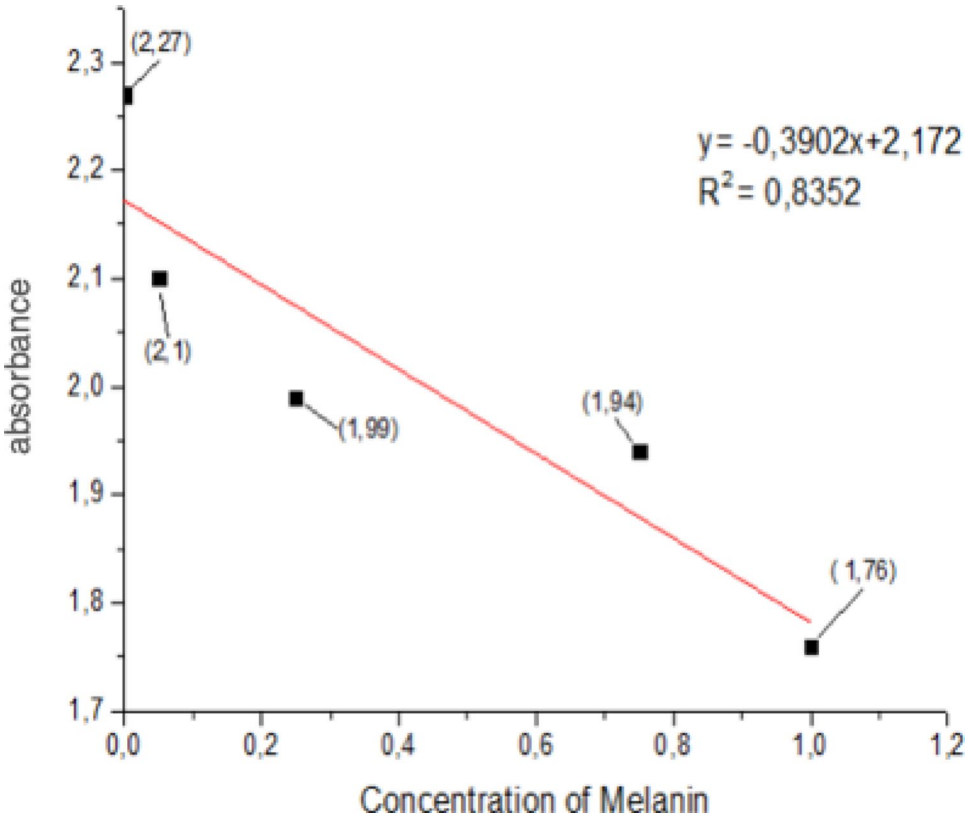


Fig. 8 Melanin concentration vs. absorbance of AuNP graph at pH 0–1 condition ($p = 0.0299$)

confidence level ($p < 0.0299$). A linear working range is important to develop sensors that can detect melanin and give concentration dependent signals. This type of sensor could potentially detect melanin concentrations in a sample, which might be useful in a variety of biological and medical applications, including assessing melanoma, evaluating pigment-related diseases and testing formulations that target skin pigmentation such as whitening agents, sunscreens, or products for tanning.

Consistent with the melanin's metal chelating ability, the interaction of AuNPs with melanin is not an unexpected outcome as well as not exclusive to AuNPs synthesized by

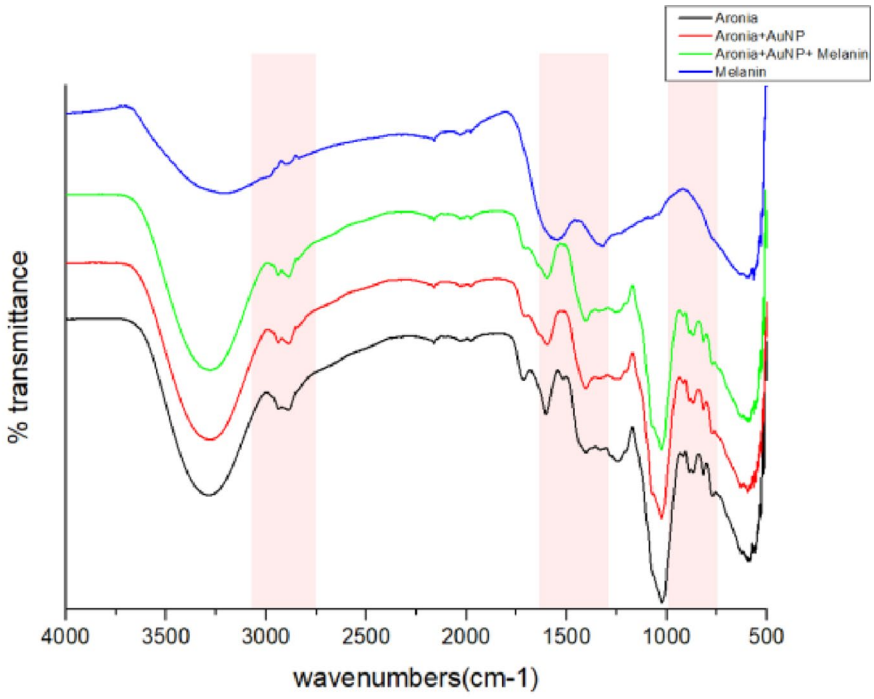


Fig. 9 FTIR Spectra of aronia extract, melanin, AuNP synthesized in aronia extract, melanin and AuNP in aronia extract

green synthesis method using *Aronia melanocarpa* extract as a reducing agent. Pornnoppadol et al. [55] utilized polydopamine-derived melanin-like nanoparticles (MNPs) as a mild reducing agent to spontaneously generate AuNPs on their surface. The article provides TEM images that clearly illustrates melanin particles decorated with a cluster of smaller gold nanoparticles, providing direct visual evidence of gold-melanin adsorption.

The interactions between AuNPs and melanin were also examined using FTIR spectroscopy (Fig. 9) to identify the functional groups involved in the interaction and to qualitatively assess possible surface interactions.

The broad band around 3300–3500 cm^{-1} in FTIR analysis of all samples corresponds to -OH groups involved in hydrogen bonding [56]. The observed prominent peak around 1600 cm^{-1}, which can be assigned to aromatic ring vibrations or C = O and/or C = C stretching vibrations which are prevalent in organic compounds with conjugated double bonds, such as phenolic compounds, aromatic rings [57]. In the Aronia+AuNPs sample, this band shows slight shift and broadening, which may suggest interaction of Aronia's aromatic or carbonyl groups to the AuNP surface. Melanin exhibits a strong peak around this region as well, consistent with aromatic C = C sytuctures and quinone-related carbonyl groups [58]. The Aronia+AuNPs+melanin sample displays a broader and more pronounced band around 1600 cm^{-1} compared to Aronia+AuNPs, which may indicate overlapping contributions from both Aronia and melanin functional groups and their possible interactions with AuNPs. Additionaly, Aronia shows characteristic bands in the 1200–1000 cm^{-1} region, attributed to C-O-C and C-O stretching vibrations of polysaccharides and phenolic glycosides [59, 60]. These bands become less distinct in the Aronia+AuNPs spectrum, possibly due to surface adsorption or hydrogen-bonding interactions with AuNPs.

4 Conclusion

This study establishes *Aronia melanocarpa* as a potent, eco-friendly and cost-effective reducing agent for the green synthesis of monodispersed gold nanoparticles (10–20 nm). Beyond demonstrating a sustainable production route, our findings reveal a significant chemical affinity between biogenic AuNPs and melanin in acidic environments. This serves as a significant foundation for detecting melanin as a biomarker in melanoma or other pigment related diseases, developing methods to test the efficacy of cosmetic formulations such as whitening agents, sunscreens, and tanning products and applications for advanced therapeutics such as photothermal therapy. Further research is still required to explore the full potential of AuNP-melanin interactions in various biomedical applications, including diagnostic tools and targeted therapies. Notably, the pH 0–1 environment, which yielded the most pronounced interactions in our study, represents an extremely acidic condition that is far from physiological relevance. However, these extreme conditions were utilized specifically to elucidate the chemical binding potential by reducing electrostatic barriers. Future work will focus on surface modification of these AuNPs to

enable similar or improved detection sensitivity at physiological pH levels. Furthermore, molecular mechanisms underlying the interaction between melanin and AuNPs remain to be elucidated.

Author Contributions Gurel Pekozer G. and Onder S. contributed to the study conception and design. Material preparation, data collection and analysis were performed by all authors. The first draft of the manuscript was written by Varol Dedecengiz G. and all authors commented on previous versions of the manuscript. All authors read and approved the final manuscript.

Funding This work was supported by TUBITAK (Turkish Scientific and Technological Research Council) under 2209 Funding Program.

Declarations

Competing Interests The authors have no relevant financial or non-financial interests to disclose.

References

1. Daraee, H., Eatemadi, A., Abbasi, E., Fekri Aval, S., Kouhi, M., & Akbarzadeh, A. (2016). Application of gold nanoparticles in biomedical and drug delivery. *Artificial Cells, Nanomedicine, and Biotechnology, 44*(1), 410–422.
2. Bahadur KC, R., Thapa, B., & Bhattarai, N. (2014). Gold nanoparticle-based gene delivery: Promises and challenges. *Nanotechnology Reviews, 3*(3), 269–280.
3. Patil, T., Gambhir, R., Vibhute, A., & Tiwari, A. P. (2023). Gold nanoparticles: Synthesis methods, functionalization and biological applications. *Journal of Cluster Science*, *34*(2), 705–725.
4. Shah, M., Badwaik, V., Kherde, Y., Waghwani, H. K., Modi, T., Aguilar, Z. P., Rodgers, H., Hamilton, W., Marutharaj, T., Webb, C., Lawrenz, M. B., & Dakshinamurthy, R. (2014). Gold nanoparticles: Various methods of synthesis and antibacterial applications. *Frontiers in Bioscience, 19*(8), 1320.
5. Oueslati, M. H., Ben Tahar, L., & Harrath, A. H. (2020). Synthesis of ultra-small gold nanoparticles by polyphenol extracted from *Salvia officinalis* and efficiency for catalytic reduction of p-nitrophenol and methylene blue. *Green Chemistry Letters and Reviews, 13*(1), 18–26.
6. Alsamhary, K., Al-Enazi, N., Alshehri, W. A., & Ameen, F. (2020). Gold nanoparticles synthesised by flavonoid tricetin as a potential antibacterial nanomedicine to treat respiratory infections causing opportunistic bacterial pathogens. *Microbial Pathogenesis, 139*, Article 103928.
7. Jha, A. K., & Prasad, K. (2012). Biosynthesis of gold nanoparticles using common aromatic plants. *International Journal of Green Nanotechnology, 4*(3), 219–224.
8. Agarwal, S., Chauhan, A., Anand, J., Abate, L., & Rai, N. (2023). *Medicinal Plant-Based alkaloids: A suitable precursor for nanoparticle synthesis and their various applications* (pp. 111–132). Secondary Metabolites from Medicinal Plants.
9. Kabak, B., Trak, D., Kendüzler, E., & Arslan, Y. (2024). Novel approach for green synthesis of stable gold nanoparticles with dried turmeric root extract: Investigations on sensor and catalytic applications. *Environmental Science and Pollution Research*, *31*(38), 50614–50629.
10. Kamala Nalini, S. P., & Vijayaraghavan, K. (2020). Green synthesis of silver and gold nanoparticles using *Aloe vera* gel and determining its antimicrobial properties on nanoparticle impregnated cotton fabric. *Journal of Nanotechnology Research, 2*(3), 42–50.
11. Yadi, M., Azizi, M., Dianat-Moghadam, H., Akbarzadeh, A., Abyadeh, M., & Milani, M. (2022). Antibacterial activity of green gold and silver nanoparticles using ginger root extract. *Bioprocess and Biosystems Engineering*, *45*(12), 1905–1917.
12. Thesing, A., Nascimento, J. E. R. D., Jacob, R. G., & Ferreira, J. (2018). Eucalyptus oil-mediated synthesis of gold nanoparticles. Journal of Chemistry and Chemical Engineering. New York. Vol. 12, no. 2 (Feb. 2018), pp. 52–59.
13. Lee, Y. J., Ahn, E. Y., & Park, Y. (2019). Shape-dependent cytotoxicity and cellular uptake of gold nanoparticles synthesized using green tea extract. *Nanoscale Research Letters*, *14*(1), 129.
14. Negreanu-Pirjol, B. S., Oprea, O. C., Negreanu-Pirjol, T., Roncea, F. N., Prelipcean, A. M., Craciunescu, O., & Popoviciu, D. R. (2023). Health benefits of antioxidant bioactive compounds in the fruits and leaves of *Lonicera caerulea* L. and *Aronia melanocarpa* (Michx.) Elliot. *Antioxidants, 12*(4), Article 951.
15. Jurendić, T., & Ščetar, M. (2021). *Aronia melanocarpa* products and by-products for health and nutrition: A review. *Antioxidants, 10*(7), Article 1052.
16. Li, S., Wang, Y., Li, T., Ma, P., Zhang, X., Xia, B., & Dong, W. (2021). Skin bioinspired anti-ultraviolet melanin/TiO 2 nanoparticles without penetration for efficient broad-spectrum sunscreen. *Colloid and Polymer Science, 299*, 1797–1805.
17. Oh, J. J., Kim, J. Y., Son, S. H., Jung, W. J., Kim, D. H., Seo, J. W., & Kim, G. H. (2021). Fungal melanin as a biocompatible broad-spectrum sunscreen with high antioxidant activity. *RSC Advances, 11*(32), 19682–19689.
18. Slominski, R. M., Sarna, T., Płonka, P. M., Raman, C., Brożyna, A. A., & Slominski, A. T. (2022). Melanoma, melanin, and melanogenesis: The Yin and Yang relationship. *Frontiers in Oncology, 12*, Article 842496.
19. Wei, H., Ren, J., Han, B., Xu, L., Han, L., & Jia, L. (2013). Stability of polydopamine and poly (DOPA) melanin-like films on the surface of polymer membranes under strongly acidic and alkaline conditions. *Colloids and Surfaces B: Biointerfaces, 110*, 22–28.
20. Liu, Y., & Simon, J. D. (2003). The effect of preparation procedures on the morphology of melanin from the ink sac of *sepia officinalis*. *Pigment Cell Research, 16*(1), 72–80.
21. Solano, F. (2020). Photoprotection and skin pigmentation: Melanin-related molecules and some other new agents obtained from natural sources. *Molecules*, *25*(7), 1537.
22. Kipalahi, S. O., Youssef, M. M., & Hamady, M. (2024). Octopus ink as a source of melanin: Preparation, evaluation, and utilization. *Alexandria Journal of Food Science and Technology, 21*(1), 1–12.
23. Chen, A., Sun, J., Liu, S., Li, L., Peng, X., Ma, L., & Zhang, R. (2020). The effect of metal ions on endogenous melanin nanoparticles used as magnetic resonance imaging contrast agents. *Biomaterials Science*, *8*(1), 379–390.
24. Fan, Q., Cheng, K., Hu, X., & Cheng, Z. (2014). Water-soluble ultrasmall melanin nanoparticle as a naturally active platform for multimodality imaging. Journal of Nuclear Medicine, 55 (supplement 1), 1073.
25. Sarna, T., Swartz, H. M., & Zadlo, A. (2022). Interaction of melanin with metal ions modulates their cytotoxic potential. *Applied Magnetic Resonance, 53*(1), 105–121.
26. Madkhali, N., & Algessair, S. (2024). Exploring the optical properties of metal-modified melanin following ultraviolet irradiation: An experimental and theoretical study using density functional theory. *Heliyon*. https://doi.org/10.1016/j.heliyon.2024.e29287
27. Kang, H. Y., Lee, J. W., Papaccio, F., Bellei, B., & Picardo, M. (2021). Alterations of the pigmentation system in the aging process. *Pigment Cell & Melanoma Research, 34*(4), 800–813.

28. Kotb El-Sayed, M. I., Abd El-Ghany, A. A., & Mohamed, R. R. (2018). Neural and endocrinal pathobiochemistry of vitiligo: Comparative study for a hypothesized mechanism. *Frontiers in Endocrinology, 9*, Article 197.
29. Schadendorf, D., Fisher, D. E., Garbe, C., Gershenwald, J. E., Grob, J. J., Halpern, A., & Hauschild, A. (2015). Melanoma. *Nature Reviews. Disease Primers, 1*(1), 1–20.
30. Rajanala, S., Maymone, M. B., & Vashi, N. A. (2019). Melasma pathogenesis: A review of the latest research, pathological findings, and investigational therapies. *Dermatology Online Journal*, 25(10).
31. Braun-Falco, O., Plewig, G., Wolff, H. H., Burgdorf, W. H., Braun-Falco, O., Plewig,G., … Burgdorf, W. H. (2000). Disorders of melanin pigmentation. dermatology, 1013–1042.
32. Krainc, T., Monje, M. H., Kinsinger, M., Bustos, B. I., & Lubbe, S. J. (2023). Melanin and neuromelanin: Linking skin pigmentation and Parkinson's disease. *Movement Disorders, 38*(2), 185–195.
33. Siddiqui, M. F., Jeon, S., & Kim, M. M. (2021). Rapid and sensitive detection of melanin using glutathione conjugated gold nanocluster based fluorescence quenching assay. *Spectrochimica Acta Part A: Molecular and Biomolecular Spectroscopy, 247*, Article 119086.
34. Jakubiak, P., Cantrill, C., Urtti, A., & Alvarez-Sánchez, R. (2019). Establishment of an in vitro–in vivo correlation for melanin binding and the extension of the ocular half-life of small-molecule drugs. *Molecular Pharmaceutics*, *16*(12), 4890–4901.
35. Verma, H. N., Singh, P., & Chavan, R. M. (2014). Gold nanoparticle: Synthesis and characterization. *Veterinary World, 7*(2), 72–77.
36. Ngumbi, P. K., Mugo, S. W., & Ngaruiya, J. M. (2018). Determination of gold nanoparticles sizes via surface plasmon resonance. *IOSR J. Appl. Chem, 11*(7), 25–29.
37. Sun, Y., & Xia, Y. (2003). Gold and silver nanoparticles: A class of chromophores with colors tunable in the range from 400 to 750 Nm. *Analyst, 128*(6), 686–691.
38. Liu, X., Yang, Y., Mao, L., Li, Z., Zhou, C., Liu, X., Zheng, S., & Hu, Y. (2015). SPR quantitative analysis of direct detection of atrazine traces on Au-nanoparticles: Nanoparticles size effect. *Sensors and Actuators. B, Chemical, 218*, 1–7.
39. Abdelhalim, M. A. K., Mady, M. M., & Ghannam, M. M. (2012). Physical properties of different gold nanoparticles: Ultraviolet-visible and fluorescence measurements. *Journal of Nanomedicine & Nanotechnology, 3*(3), 178–194.
40. Devi, S., Singh, B., Paul, A. K., & Tyagi, S. (2016). Highly sensitive and selective detection of trinitrotoluene using cysteine-capped gold nanoparticles. *Analytical Methods, 8*(22), 4398–4405.
41. Mock, J. J., Smith, D. R., & Schultz, S. (2003). Local refractive index dependence of plasmon resonance spectra from individual nanoparticles. *Nano Letters, 3*(4), 485–491.
42. Ghosh, S. K., & Pal, T. (2007). Interparticle coupling effect on the surface plasmon resonance of gold nanoparticles: From theory to applications. *Chemical Reviews, 107*(11), 4797–4862.
43. Li, D. D., Gu, X., Timchenko, V., Chan, Q. N., Yuen, A. C., & Yeoh, G. H. (2018). Study of morphology and optical properties of gold nanoparticle aggregates under different pH conditions. *Langmuir, 34*(35), 10340–10352.
44. Velgosova, O., Mikulková, Z., & Lisnichuk, M. (2025). The influence of precursor pH on the synthesis and morphology of AuNPs synthesized using green tea leaf extract. *Crystals*, *15*(8), 682.
45. Rahman, M. R., Saleh, F. S., Okajima, T., & Ohsaka, T. (2011). pH dependence of the size and crystallographic orientation of the gold nanoparticles prepared by seed-mediated growth. *Langmuir, 27*(8), 5126–5135.
46. Yazdani, S., Daneshkhah, A., Diwate, A., Patel, H., Smith, J., & Reul, O. (2021). Model for gold nanoparticle synthesis: Effect of pH and reaction time. *ACS Omega*, *6*, 16847–16853.
47. Thanh, N. T., Maclean, N., & Mahiddine, S. (2014). Mechanisms of nucleation and growth of nanoparticles in solution. *Chemical Reviews, 114*(15), 7610–7630.
48. Sidhu, A. K., Verma, N., & Kaushal, P. (2022). Role of biogenic capping agents in the synthesis of metallic nanoparticles and evaluation of their therapeutic potential. *Frontiers in Nanotechnology, 3*, Article 801620.
49. Javed, R., Zia, M., Naz, S., Aisida, S. O., Ain, N. U., & Ao, Q. (2020). Role of capping agents in the application of nanoparticles in biomedicine and environmental remediation: Recent trends and future prospects. *Journal of Nanobiotechnology, 18*(1), Article 172.
50. Pirsaheb, M., Gholami, T., Seifi, H., Dawi, E. A., Said, E. A., Hamoody, A. H. M.,… Salavati-Niasari, M. (2024). Green synthesis of nanomaterials by using plant extracts as reducing and capping agents. Environmental Science and Pollution Research, 31(17),24768–24787.
51. Husseiny, M. I., Abd El-Aziz, M., Badr, Y., & Mahmoud, M. A. (2007). Biosynthesis of gold nanoparticles using *Pseudomonas aeruginosa*. *Spectrochimica Acta. Part A, Molecular and Biomolecular Spectroscopy, 67*(3–4), 1003–1006.
52. Ankamwar, B. (2010). Biosynthesis of gold nanoparticles (green-gold) using leaf extract of *terminalia catappa*. *Journal of Chemistry, 7*(4), 1334–1339.
53. da Silva, M. P., Fernandes, J. C., de Figueiredo, N. B., Congiu, M., Mulato, M., & Graeff, C. (2014). Melanin as an active layer in biosensors. *AIP Advances, 4*(3), Article 037120.
54. Costa, T. G., Younger, R., Poe, C., Farmer, P. J., & Szpoganicz, B. (2012). Studies on synthetic and natural melanin and its affinity for Fe(III) ion. *Bioinorganic Chemistry and Applications, 2012*, Article 712840.
55. Pornnoppadol, G., Cho, S., Yu, J. H., Kim, S. H., & Nam, Y. S. (2024). Cancer-targeting gold-decorated melanin nanoparticles for in vivo near-infrared photothermal therapy. *Molecular Systems Design & Engineering, 9*(5), 507–517.
56. Farhat, I. A., Orset, S., Moreau, P., & Blanshard, J. M. (1998). FTIR study of hydration phenomena in protein–sugar systems. *Journal of Colloid and Interface Science*, *207*(2), 200–208.
57. Janković, B., Marinović-Cincović, M., & Janković, M. (2016). TG-DTA-FTIR analysis and isoconversional reaction profiles for thermal and thermo-oxidative degradation processes in black chokeberry (*aroniamelanocarpa*). *Chemical Papers, 70*(8), 1094–1105.
58. Shaju, P. M., Ganesan, P., Kingston, S. D., & Muruganantham, M. (2022). Fourier transform Infrared characterization of melanin free ink from selected cephalopods for identification of active functional groups responsible for antioxidant activity. *Journal of the Indian Chemical Society, 99*(3), Article 100375.
59. Neagu, M., Pascu, D. E., Traistaru, G. A., Cretu, G., Nechifor, A. C., Bunaciu, A. A., & Aboul-Enein, H. Y. (2013). Membrane separation and concentration study of biological active compounds. *Analytical Chemistry Letters, 3*(5–6), 314–321.
60. Wang, J., Wang, J., Hao, J., Jiang, M., Zhao, C., & Fan, Z. (2024). Antioxidant activity and structural characterization of anthocyanin–polysaccharide complexes from *Aronia melanocarpa*. *International Journal of Molecular Sciences, 25*(24), 13347.

Publisher's Note Springer Nature remains neutral with regard to jurisdictional claims in published maps and institutional affiliations.

Springer Nature or its licensor (e.g. a society or other partner) holds exclusive rights to this article under a publishing agreement with the author(s) or other rightsholder(s); author self-archiving of the accepted manuscript version of this article is solely governed by the terms of such publishing agreement and applicable law.